Characterization of the Membrane Domain Subunit NuoJ (ND6) of the NADH-Quinone Oxidoreductase from *Escherichia coli* by Chromosomal DNA Manipulation†

Mou-Chieh Kao,‡ Salvatore Di Bernardo,‡ Eiko Nakamaru-Ogiso,‡ Hideto Miyoshi,‖ Akemi Matsuno-Yagi,*,‡ and Takao Yagi*,‡

Division of Biochemistry, Department of Molecular and Experimental Medicine, The Scripps Research Institute, 10550 North Torrey Pines Road, La Jolla, California 92037, and Division of Applied Life Sciences, Graduate School of Agriculture, Kyoto University, Kyoto 606-8502, Japan

Received November 5, 2004

ABSTRACT: The ND6 subunit is one of seven mitochondrial DNA-encoded subunits of the proton-translocating NADH-quinone oxidoreductase (complex I). Physiological importance of the ND6 subunit is becoming increasingly apparent because a number of mutations leading to amino acid changes in this subunit have been found to be associated with known mitochondrial diseases. Using the *Escherichia coli* enzyme (NDH-1), we have investigated the NuoJ subunit (the *E. coli* counterpart of ND6) by employing a chromosomal DNA manipulation technique. A series of point mutations was constructed directly on the *nuoJ* gene in the chromosome targeting at highly conserved residues. Analyses with blue-native gel electrophoresis and immunological methods revealed that, in all point mutants, the assembly of NDH-1 was normal and that the deamino-NADH-$K_3Fe(CN)_6$ reductase activity of the membrane was essentially the same as that of the wild-type. However, energy-coupled NDH-1 activities were affected to varied extents. Among them, mutants of the Val-65 residue that is located in the most conserved transmembrane segment significantly lost the coupled electron-transfer activities and exhibited diminished membrane potential and proton translocation. This may suggest that Val-65 or the area around it is important for energy transduction of the coupling site 1. Together with the results on mutations related to human diseases, possible functional roles of the NuoJ subunit have been discussed.

Mammalian complex I is the largest, most complicated, and least understood of the respiratory complexes (*1*). It consists of at least 46 different subunits, with a molecular mass of ∼1000 kDa. In contrast, the bacterial H^+-translocating NADH-quinone oxidoreductase (NDH-1),[1] which is equivalent of complex I, is simpler and contains 14 subunits (designated Nqo1−14 for *Paracoccus denitrificans* and *Thermus thermophilus* and NuoA-N for *E. coli*)[2] (*2*, *3*). All of them are homologues of the subunits of the mitochondrial core enzyme, including the seven mitochondrially encoded ND subunits. NDH-1/complex I represents the first membrane-bound electron transport complex of the respiratory chain and is responsible for coupling the transfer of two electrons from NADH to quinone with the translocation of four protons across the membrane to generate a membrane potential and proton gradient for ATP synthesis (*1*).

Electron microscopy revealed that the bacterial NDH-1 has an L-shaped structure with a peripheral arm and a membrane arm (*4*). The peripheral arm protrudes into the cytoplasm, bears the binding site for NADH, and contains all known cofactors including one FMN and eight to nine iron−sulfur clusters (*5*, *6*). This arm consists of seven subunits (NuoB, -C, -D, -E, -F, -G, and -I). In *E. coli*, the NuoC (30 kDa) and NuoD (49 kDa) subunits are fused to give a single subunit (NuoCD) (*7*). Among these peripheral subunits, the NuoB (PSST) and NuoI (TYKY) have been experimentally demonstrated to act like a connector between the peripheral and the membrane arms (*8*−*10*). The membrane arm is embedded within the cytoplasmic membrane and is also made up of seven subunits (NuoA, -H, -J, -K, -L, -M, and -N) (*11*−*13*), which are homologues of mtDNA-

† This work was supported by U.S. Public Health Service Grant R01GM33712 (A.M.-Y. and T.Y.). Synthesis of oligonucleotides and DNA sequencing were, in part, supported by the Sam and Rose Stein Endowment Fund.

* To whom correspondence should be addressed. (T.Y.) Phone: (858) 784-8094; fax: (858) 784-2054; e-mail: yagi@scripps.edu. (A.M.-Y.) Phone: (858) 784-2596; e-mail: yagi2@scripps.edu.

‡ The Scripps Research Institute.

‖ Kyoto University.

[1] Abbreviations: NDH-1, bacterial H^+ (Na^+)-translocating NADH-quinone oxidoreductase; complex I, mitochondrial H^+-translocating NADH-quinone oxidoreductase; NDH-2, bacterial NADH-quinone oxidoreductase lacking the energy coupling site; DB, dimethoxy-5-methyl-6-decyl-1,4-benzoquinone; dNADH, reduced nicotinamide hypoxanthine dinucleotide (deamino-NADH); Spc, spectinomycin; PCR, polymerase chain reaction; EDTA, ethylenediaminetetraacetic acid; PMSF, phenylmethanesulfonyl fluoride; DTT, dithiothreitol; Q, quinone(s); LHON, Leber's hereditary optic neuropathy; cap-40, capsaicin-40; Bistris, 2-[bis(2-hydroxyethyl)amino]-2-(hydroxymethyl)propane-1,3-diol; MOPS, 3-(*N*-morpholino)propane-sulfonic acid; oxonol VI, bis-(3-propyl-5-oxoisoxazol-4-yl)pentamethine oxonol; ACMA, 9-amino-6-chloro-2-methoxyacridine; FCCP, carbonyl cyanide *p*-trifluoromethoxyphenylhydrazone; TM, transmembrane.

[2] For simplicity, the *E. coli* terminology was mainly used throughout this paper. Bovine naming was also used as needed for clarity.

10.1021/bi0476477 CCC: $30.25
Published on Web 02/10/2005

encoded subunits (ND1−6 and ND4L) (*14*, *15*). Unlike the peripheral arm, no known prosthetic group has been found in the membrane arm. Despite the knowledge of the primary structure, very limited information is available about the functional properties and the arrangement of these membrane-bound subunits. However, it is generally believed that the membrane arm participates in H^+ (or Na^+) translocation and quinone and inhibitor binding (*16*−*18*).

Recently, human complex I, especially the mitochondrially encoded subunits, has increasing medical importance because mutations of the mtDNA have been shown to cause a wide variety of human degenerative diseases (*19*). Among those mtDNA-encoded complex I subunits, ND6 is of particular interest because it has been recognized recently that the *ND6* gene of complex I is a hot spot for pathogenic mutations (*20*). Numerous point mutations leading to amino acid changes in this subunit have been found to be associated with known mitochondrial diseases such as Leber's hereditary optic neuropathy (LHON) (*21*). In addition to pathogenic mutations, the analyses of frameshift mutations in a mouse cell line (*22*) and in the unicellular green alga *Chlamydomonas reinhardtii* (*23*) have shown that the ND6 subunit is essential for the assembly of complex I. Furthermore, the ND6 subunit has been suspected to be involved in the quinone redox site in the membrane-buried portion of the complex (*20*).

Previously, we experimentally determined the topology of the *Paracoccus* NuoJ subunit (*13*). The *Paracoccus* NuoJ subunit consists of five transmembrane segments (named TM1−5 from the N- to the C-terminus) with the N- and C-terminal regions directed toward the periplasmic and cytoplasmic sides of the membrane, respectively. Interestingly, examination of the proposed NuoJ model reveals that all of the pathogenic mutations related to human ND6 gene and conserved residues appear within or near the TM2 and TM3. Therefore, it is tempting to suspect that this region of the NuoJ subunit plays an important role in the catalytic function or structural arrangement of complex I. At present, it seems extremely difficult to perform systematic manipulation of mitochondrial DNA. We chose *E. coli* NuoJ as the model system because gene manipulation techniques are much more advanced and well-developed in this bacterium. According to sequence alignments and topological predictions derived from a variety of computer programs (see Results), the topology of *E. coli* NuoJ subunit is akin to its counterpart of *Paracoccus*. By direct introduction of mutations in the *E. coli* chromosomal NDH-1 operon, we constructed a series of mutants carrying point mutations on conserved residues and characterized these mutants.

EXPERIMENTAL PROCEDURES

Materials. The pCRScript Cloning kit was from Stratagene (La Jolla, CA). Site-specific mutants were constructed using the GeneEditor Mutagenesis Kit from Promega (Madison, WI). The gene replacement vector, pKO3, was a generous gift from Dr. George M. Church (Harvard Medical School, Boston, MA). Materials for PCR product purification, gel extraction, and plasmid preparation were obtained from Qiagen (Valencia, CA). Bis-(3-propyl-5-oxoisoxazol-4-yl)-pentamethine oxonol (oxonol VI) and 9-amino-6-chloro-2-methoxyacridine (ACMA) were obtained from Molecular Probes (Eugene, OR). The BCA protein assay kit, Super-Signal West Pico chemiluminescent substrate, and Imject Activated Immunogen Conjugation kit were from Pierce (Rockford, IL). dNADH, DB, chloramphenicol, and spectinomycin (Spc) were from Sigma (St. Louis, MO). All other materials were reagent grade and obtained from commercial sources.

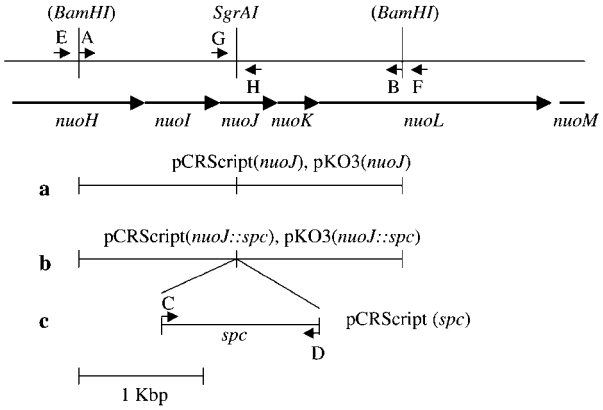

FIGURE 1: Schematic representation of the strategy of *nuoJ* cloning, insertion of a Spc cassette in the *E. coli nuoJ* gene, and construction of site-specific *nuoJ* mutants. Arrows (A−H) illustrate the primers used in this study. The restriction enzymes in the parentheses are newly introduced into the *E. coli* DNA.

Cloning and Mutagenesis of the E. coli nuoJ Gene. The vectors constructed in this study are shown in Figure 1. The gene encoding the NuoJ subunit together with a 1 kb DNA segment upstream and a 1 kb DNA segment downstream were amplified from *E. coli* DH5α using PCR. To generate the *Bam*HI restriction site on both ends of the cloned fragment, primer A (5′-GCATGTGT*GGATCC*TTATCCCG-CAATTC -3′) and primer B (5′-GTCTGCAAC*GGATCC*T-GCGCAGATTTAC-3′) were used, where the italicized bases represented the restriction site sequence and the underlined bases were altered from *E. coli*. The spectinomycin-encoding gene from transposon Tn554 of *Staphylococcus aureus* (*24*) was obtained by PCR amplification using the sense primer C (5′-*CGCCGGTG*GAACGAAAACTCACGTTAAG-3′) and the antisense primer D (5′-*CACCGGCG*CTTTCTATTTTC-AATAGTTAC-3′) both containing a *Sgr*AI restriction site represented by italicized bases. The *nuoJ*-containing fragment and the Spc cassette were individually subcloned into pPCR-Script Amp SK(+), and their sequences were verified by sequencing. The resulting plasmids were designated pCR-Script(*nuoJ*) and pCRScript(*spc*), respectively (Figure 1a,c).

To introduce a site-specific mutation into the *nuoJ* gene of the *E. coli* NDH-1 operon, creation of a *nuoJ* gene knock-out mutant was a prerequisite. We have adopted the pKO3 system developed by Link et al. (*25*) that is based on homologous recombination. In this gene replacement system, the pKO3 vector employed contains a *repA*(Ts) (temperature sensitive replication origin), a chloramphenicol-resistant gene (*cat*), and a *Bacillus subtilis sacB* gene encoding levansucrase. The pKO3 carrying NuoJ knock-out DNA was prepared as follows. Because the *E. coli nuoJ* contains one endogenous *Sgr*AI site approximately one-third from the beginning of the gene, a *Sgr*AI−*Sgr*AI fragment carrying a Spc cassette can be inserted into *E. coli nuoJ* without introduction of new restriction sites. On the basis of this, the pCRScript(*spc*) was digested with *Sgr*AI, and the DNA

Table 1: Primers for Introduction of a Site-Specific Mutation into *E. coli* NuoJ Subunit

mutation	mutagenic primer sequence[a]
Y59C	5′-ATTATCGTCTGCGCGGGTGCCATTATG-3′
Y59F	5′-ATTATCGTCTTCGCGGGTGCCATTATG-3′
G61V	5′-CGTCTACGCGGTTGCCATTATGGTG-3′
G61L	5′-CGTCTACGCGCT TGCCATTATGGTG-3′
M64V	5′-GGTGCCATTGTGGTGCTGTTCGTG-3′
M64I	5′-GGTGCCATTATAGTGCTGTTCGTGTTC-3′
V65G	5′-TGCCATTATGGGACTGTTCGTGTTC-3′
V65L	5′-TGCCATTATGCTGCTGTTCGTGTTCG-3′
F67A	5′-TTATGGTGCTGGCCGTGTTCGTGGTG-3′
E80Q	5′-TGGGCGGTTCACAAATCGAACAGG-3′
E80A	5′-TGGGCGGTTCAGCAATCGAACAGG-3′

[a] Underline indicates mutation.

fragment containing Spc cassette was then purified and ligated into the *Sgr*AI-digested pCRScript(*nuoJ*). The plasmid thus obtained was named pCRScript (*nuoJ*::*spc*) (Figure 1b). A *Bam*HI−*Bam*HI fragment of this construct was then cloned into the *Bam*HI site of pKO3, yielding pKO3(*nuoJ*::*spc*).

The pKO3 vectors carrying mutated *nuoJ* genes were prepared as shown in Figure 1. First, the pCRScript(*nuoJ*) was used as the template to generate *nuoJ* point mutations. The pCRScript(*nuoJ*) was mutagenized with synthetic oligonucleotides listed in Table 1 using the GeneEditor in vitro site-directed mutagenesis system (Promega) according to the manufacturer's instructions. All mutated *nuoJ* genes were verified by DNA sequencing using primer G (5′-TGATAGCCATACTTGCGACCTTG-3′) and/or primer H (5′-AGCGTAATACCCACTGCTTTAGC-3′). These two primers are located inside the *nuoJ* gene flanking the intended mutation sites. Each DNA fragment containing the desired *nuoJ* mutation was then isolated by *Bam*HI digestion from the pCRScript constructs and transferred to integration plasmid pKO3 at the *Bam*HI site. The resulting plasmids were referred to as pKO3(*nuoJ* mutants). When the *Bam*HI−*Bam*HI fragment directly derived from pCRScript(*nuoJ*) that contained the wild-type *nuoJ* gene without any mutation was inserted into the *Bam*HI site of pKO3, the construct was named pKO3(*nuoJ*).

Preparation of Knock-Out and Mutant Cells. The knock-out allele cloned into the pKO3 gene replacement vector (i.e., pKO3(*nuoJ*::*spc*)) was used to transform *E. coli* strain MC4100 (*F*$^-$, *araD139*, Δ(*arg F-lac*)*U169*, *ptsF25*, *relA1*, *flb5301*, *rpsL 150.λ*$^-$), and homologous recombination was performed according to Link et al. (*25*) with some minor modifications as described previously (*26*). The correct generation of the chromosomal NuoJ knock-out mutant by insertion of a Spc cassette in the *nuoJ* gene was verified by PCR amplification using primer E (5′-TGTTCCTCGGGCTTTCCTTGATG-3′) and primer D or primers C and F (5′-TACCATGGTTGCGGCGTGGATC-3′). Primers E and F were complementary to upstream and downstream of the cloned *E. coli* chromosome, respectively, and primers C and D were located within the Spc cassette. With this design, not only the presence of the Spc cassette but also its location in the genomic DNA was confirmed. The NuoJ knock-out MC4100 cells were stored as glycerol stocks at − 80 °C. The NuoJ knock-out MC4100 competent cells were then applied to introduce *nuoJ* mutated DNA in the *E. coli* genome using a similar procedure except that the identification of recombinants was carried out by screening for spectinomycin sensitivity in addition to chloramphenicol sensitivity. To demonstrate that the gene replacement procedure used in this study did not introduce polar effects in the point mutants, we have created a control mutant (KO-rev) that employed unmutated gene pKO3(*nuoJ*), instead of pKO3(*nuoJ* mutants), in the recombination process.

To confirm the presence of the mutations, the sense primer E and the antisense primer H were applied in colony PCR to amplify *nuoJ*-containing DNA fragments. The obtained *nuoJ* DNA fragments were then subjected to direct sequencing using primer G.

Antibody Production. An oligopeptide, H-CDSAKRK-TEEHA-OH (designated NuoJc), derived from the C-terminal region of the *E. coli* NuoJ subunit with an additional cysteine incorporated for the purpose of conjugation was linked to maleimide-activated bovine serum albumin (Pierce, Rockford, IL) as an immunogen according to the manufacturer's protocol. Antibodies against C-terminal regions of *E. coli* NuoA and NuoK subunits (designated NuoAc and NuoKc, respectively) had been produced by the similar procedure as reported earlier (*26*). The NuoB-, NuoCD-, NuoE-, NuoF-, NuoG-, and NuoI-specific antibodies were raised in rabbits against the whole subunit as described previously (*5*, *27*). The antibodies were affinity-purified according to Han et al. (*28*).

Bacterial Growth and Membrane Preparation. Cells were first grown in 3 mL of LB medium from glycerol stocks at 37 °C for 10 h. Five hundred microliters of the culture was used to inoculate 250 mL of terrific broth (TB), and cells were cultivated at 30 °C with shaking until A_{600} was ∼2. The cells were then harvested in a SLA-1500 rotor at 6000 rpm for 10 min. The cell pellet was resuspended at 10% (w/v) in a buffer containing 10 mM Tris-HCl (pH 7.0), 1 mM EDTA, 1 mM DTT, 1 mM PMSF, and 15% (w/v) glycerol. The cell suspension was then passed through the French press once at 25 000 psi. After cell debris was removed by centrifugation in a Sorvall SS34 rotor at 12000 rpm for 10 min, the supernatant was further ultracentrifuged at 50 000 rpm for 30 min in a Beckman Spinco 60Ti rotor. The collected pellets were resuspended in the same buffer, and the resulting membrane suspension was used immediately for enzyme assays or stored in small aliquots at −80 °C for later use.

Gel Electrophoresis and Immunoblotting Analysis. Ten micrograms of protein from each membrane suspension was first subjected to SDS−PAGE using the discontinuous system of Laemmli (*29*). Western blotting experiments were then conducted to investigate the expression of individual NDH-1 subunit in the knock-out and point mutants. Antibodies against the membrane domain subunits NuoJc, NuoKc, and NuoAc and the peripheral subunits NuoCD, NuoE, NuoF, NuoG, NuoB, and NuoI recognized a band in the *E. coli* membranes with an apparent molecular mass of 21, 11, 16, 65, 20, 50, 91, 22, and 21 kDa, respectively.

To evaluate the assembly of NDH-1, membrane samples were subjected to blue-native (BN)-PAGE according to Schägger and von Jagow (*30*) in the mini-gel format (Bio-Rad). The *E. coli* membrane samples equivalent to 800 μg of protein were resuspended in 40 μL of 50 mM Bistris-HCl (pH 7.0) buffer containing 750 mM aminocaproic acid, followed by addition of 6 μL of 10% (w/v) *n*-dodecyl-β-

maltoside and 50 μg/mL DNase for membrane solubilization. After incubation on ice for 3 h, the samples were centrifuged at 149 000*g* in a Beckman Airfuge for 10 min. The supernatant was collected (~40 μL), and glycerol was added to a final concentration of 15% to facilitate sample application. Shortly before running BN-PAGE, 8 μL of 5% Coomassie blue in 500 mM aminocaproic acid was added to the samples. Ten microliters of the previous samples were then loaded into a 7% separating gel with a 4% stacking gel, and BN-PAGE was performed in the cold room at 80 V until entry of the protein sample into the separating gel. Before the electrophoresis was continued at 200 V for 3 h, the cathode buffer containing 0.02% Serva Blue G was replaced by the same buffer but with 0.002% dye. Immediately after electrophoresis, the gel was washed several times in 2 mM Tris-HCl (pH 7.5) buffer and then subjected to immunoblotting analyses. Immunodetection was performed using affinity-purified antibody specific for NuoB, NuoI, or NuoAc.

Enzymatic Assay. It is well-known that NDH-1/complex I and NDH-2 can be distinguished by use of dNADH because only the former can utilize this substrate (*31*). Therefore, we have used dNADH as the substrate throughout this study. Measurements of enzymatic activity were carried out at 37 °C using a SLM DW-2000 spectrophotometer. The dNADH oxidase activity was assayed at 340 nm in 10 mM potassium phosphate (pH 7.0) buffer containing 1 mM EDTA with the addition of 0.15 mM dNADH as described in (*32*), using the *E. coli* membranes (80 μg of protein/mL). Nearly complete inhibition of this reaction was achieved by addition of 10 μM cap-40 (*33*). The dNADH-DB reductase activity measurements were conducted similarly, except that 10 mM KCN and 100 μM DB were also included in the assay mixture. The dNADH-$K_3Fe(CN)_6$ reductase activity was measured at 420 nm in the same buffer in the presence of 10 mM KCN, 0.15 mM dNADH, and 1 mM $K_3Fe(CN)_6$. Nonenzymatic reaction of dNADH-$K_3Fe(CN)_6$ was subtracted from all measurements. The extinction coefficients used for activity calculations were $\epsilon_{340} = 6.22$ mM^{-1} cm^{-1} for dNADH and $\epsilon_{420} = 1.00$ mM^{-1} cm^{-1} for $K_3Fe(CN)_6$.

Membrane Potential Measurement. The generation of membrane potential by the NuoJ mutants was monitored optically with the indicator dye oxonol VI. The standard reaction mixture contained 50 mM MOPS (pH 7.3), 10 mM $MgCl_2$, 50 mM KCl, 2 μM oxonol VI, and the *E. coli* membrane samples (400 μg of protein/mL). After the signal had stabilized, the reaction was started by addition of 0.2 mM dNADH. $\Delta\Psi$-induced absorbance change was monitored at 630 minus 603 nm using a DW-2000 dual wavelength spectrophotometer at 37 °C. When desired, the proton ionophore FCCP, potassium ionophore valinomycin, and electroneutral K^+/H^+ exchanger nigericin were added to a final concentration of 2, 2, and 0.2 μM, respectively.

Fluorescence Assay for Proton Translocation. Proton-pumping activity of NDH-1 was estimated from ACMA fluorescence quenching as described by Amarneh and Vik (*34*). The reaction mixture was the same as that for oxonol VI assay except that oxonol VI was replaced with 2 μM ACMA, and the *E. coli* membrane samples were added at 150 μg of protein/mL. The reaction was initiated by adding 0.2 mM dNADH. The fluorescence was recorded at room temperature using a SpectraMax M2 fluorescence microplate reader (Molecular Devices Corp.) with an excitation wavelength of 410 nm and an emission wavelength of 480 nm. When appropriate, FCCP, valinomycin, and nigericin were added to a final concentration of 10, 2, and 2 μM, respectively.

Other Analytical Procedures. Protein concentrations were determined by the BCA protein assay kit (Pierce) using bovine serum albumin as the standard according to the manufacturer's instruction. Any variations from the procedures and other details are described in the figure legends.

RESULTS

Sequence Analysis of the NuoJ Subunit. The NuoJ/Nqo10/ND6 subunit is one of the less evolutionarily conserved NDH-1/complex I subunits (*35*). Figure 2A shows the amino acid sequence alignment of this subunit from various organisms including mammals, fungi, and bacteria. Figure 2B is a proposed topology of the *E. coli* NuoJ subunit derived from topological studies of the *P. denitrificans* NuoJ subunit (*13*), together with predictions offered by a variety of computer programs including TMHMM (*36*), HMMTOP (*37*), TopPred2 (*38*), and TMpred (*39*). According to this proposed model, the *E. coli* NuoJ subunit contains five defined hydrophobic stretches corresponding to transmembrane segments (named TM1−5 from the N-terminus), with the N- and C-terminal regions facing the periplasmic and cytoplasmic sides of the membrane, respectively. By searching sequence databases and aligning primary sequences of NuoJ homologues available to date, we identified five residues that are well-conserved in this subunit (marked with gray boxes in Figure 2A). Of those residues, Tyr-59, Gly-61, Val-65, and Phe-67 (*E. coli* numbering) are located in the TM3, and Glu80 is in a cytoplasmic loop immediately after TM3. TM3 represents the most phylogenetically conserved part of this subunit. In addition, there are eight residues that are known to be associated with pathogenic mutations, and six of them are located within TM3 or in its vicinity (arrows in Figure 2A). Among the pathogenic mutations, M64V (both human and *E. coli* numbering) is considered as the primary mutation for LHON. It is, therefore, likely that the area encompassing TM3 is critically important in the NuoJ subunit, and we selected TM3 as the main target of the investigation. Because the membrane domain of NDH-1 is likely to participate in proton translocation, residues capable of protonation may be of particular interest. From this point of view, Tyr-59 is a good candidate for the study because this residue is almost perfectly conserved among homologues of NuoJ currently available in sequence databases, and the corresponding position in human ND6 is associated with LHON.

To clarify the structural and functional roles of the conserved residues as well as residues corresponding to those linked to human diseases, we have generated a series of point mutants, including Y59C, Y59F, G61V, G61L, M64V, M64I, V65G, V65L, F67A, E80Q, and E80A, using homologous recombination targeted directly at chromosome. The existence of these mutations was confirmed by DNA sequencing analyses.

Subunit Assembly of NDH-1 in NuoJ Mutations. To investigate whether mutation of the NuoJ subunit causes incomplete assembly of NDH-1, we have performed BN−

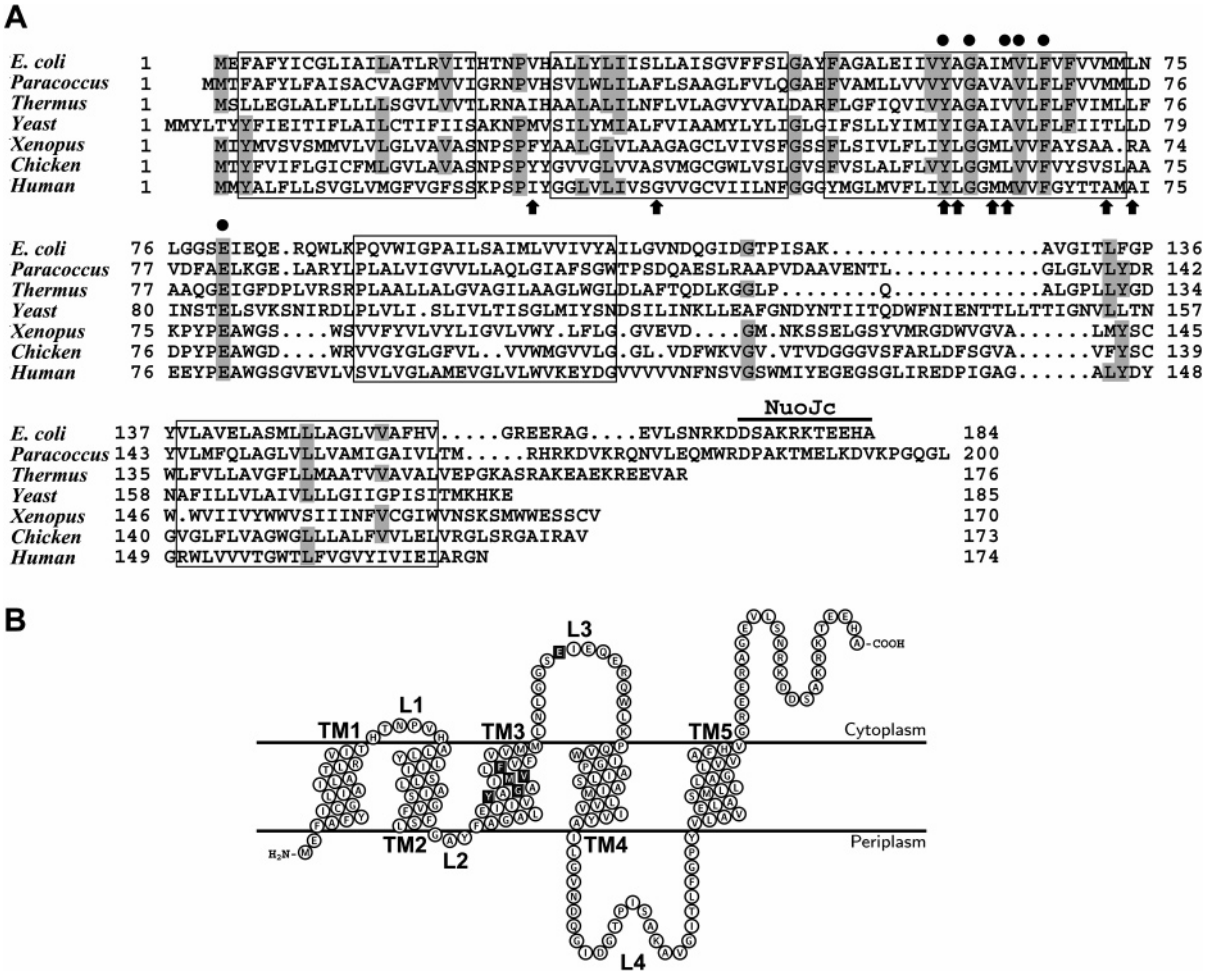

FIGURE 2: (A) Comparison of the deduced amino acid sequence of the *E. coli* NuoJ subunit with its homologues from various organisms. The alignment was conducted with the PILEUP programs of GCG software (*46*). Conserved residues are highlighted by gray boxes. Sequence sources and their Swiss-Prot accession numbers are (from top to bottom): *E. coli* K-12 [P33605], *P. denitrificans* [P29922], *T. thermophilus* HB-8 [Q56225], yeast *Yarrowia lipolytica* [Q9B6E9], *Xenopus laevis* [P03927], chicken *Gallus gallus* [P18941], and *Homo sapiens* [P03923]. Amino acid residues mutated in this study are marked by black dots. Five predicted transmembrane segments (TM1−5) are surrounded by blocks according to Kao et al. (*13*). The segment marked NuoJc indicates the oligopeptide region used to raise the antibody specific to the C-terminal region of the *E. coli* NuoJ. The amino acid residues reported for pathogenic point mutations in the human mitochondrial ND6 subunit are marked by arrows. (B) Proposed topology of the *E. coli* NuoJ subunit. The prediction has been performed on the basis of the reported topology of its *Paracoccus* counterpart (*13*). As described in the Results, the five transmembrane segments of the *E. coli* NuoJ subunit from the N- to the C-terminus are tentatively designated TM1−TM5. The loops are designated L1−L4. The N- and C-terminus of the subunit are exposed to the periplasmic side and the cytoplasmic side of the membrane, respectively. The mutated amino acid residues are displayed by black squares.

PAGE analysis of the constructed mutants. Unlike SDS−PAGE, which denatures and separates enzyme complexes into individual subunits, BN−PAGE maintains enzyme complexes in their intact forms so that the amount of the fully assembled NDH-1 can be estimated by immunoblotting using an antibody specific to one of its component subunits. In Figure 3, the assembled NDH-1 on a BN−PAGE gel of our samples was visualized by using anti-NuoB antibody. The NuoJ knock-out mutant apparently lacked a fully assembled complex (see next paragraph for details). However, the revertant mutant (KO-rev) and all 11 point mutants showed the same level of the assembled NDH-1 as that of the wild-type. Similar results were obtained when anti-NuoI antibody or anti-NuoA antibody was used for detection (data not shown). Apparently, none of the point mutations affected the assembly of the NDH-1 complex.

To confirm the assembly status and to investigate the individual subunits of the NDH-1, we analyzed mutant *E. coli* membranes on SDS−PAGE by immunoblotting with subunit-specific antibodies (Figure 4). For this purpose, we have used antibodies available to date, which included six antibodies against subunits located in the peripheral domain (NuoB, NuoCD, NuoE, NuoF, NuoG, and NuoI) and three antibodies against subunits present in the membrane domain (NuoA, NuoJ, and NuoK). The NuoJ knock-out mutant, as expected, entirely lacked NuoJ. It also showed diminished amounts of other subunits, presumably due to incomplete assembly of the whole complex. In the revertant mutant (KO-rev), all subunits existed at the same levels as the wild-type. Similarly, as for the 11 constructed point mutants, no significant quantitative difference was observed for the nine NDH-1 subunits tested. In addition, all mutated NuoJ subunit exhibited the same electrophoretic mobility as the wild-type, suggesting that these mutations did not result in an unstable or truncated NuoJ subunit. Taken together, our results indicate that there is no drastic change that may alter the assembly status of the NDH-1 in any of the point mutants constructed in this study.

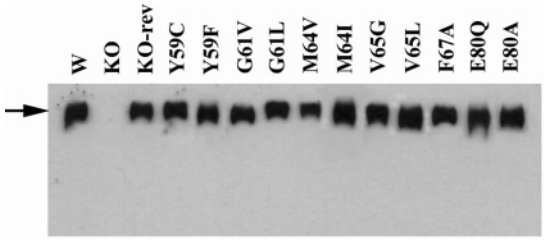

FIGURE 3: Immunoblotting of the blue-native polyacrylamide gels of membrane preparations from the *E. coli* wild-type (W), NuoJ knock-out (KO), NuoJ revertant (KO-rev), and NuoJ point mutants by using the affinity-purified antibody specific to the *E. coli* NuoB subunit. The electrophoresis was performed as described in Experimental Procedures. After blue-native polyacrylamide gel electrophoresis, the *E. coli* membrane proteins were transferred to nitrocellulose membranes. Subsequently, the nitrocellulose membranes were immunostained with the affinity-purified NuoB antibody using SuperSignal West Pico system (Pierce) according to Han et al. (*28*). The secondary antibody used for detection was goat anti-rabbit IgG horseradish peroxidase conjugate (Pierce). The arrow shows the location of the immunoblotting band recognized by the anti-NuoB antibody.

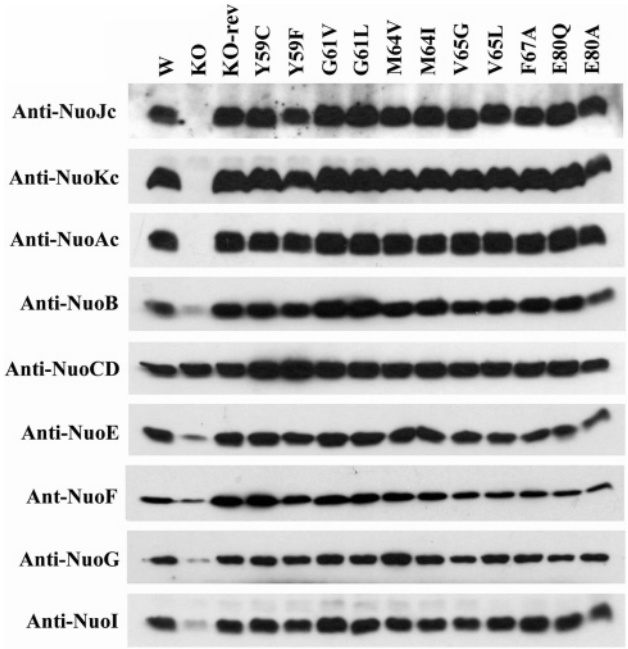

FIGURE 4: Immunoblotting of membrane preparations from the wild-type (W), NuoJ knock-out (KO), NuoJ revertant (KO-rev), and site-specific NuoJ mutants by using antibodies specific to the NuoJc, NuoKc, NuoAc, NuoB, NuoCD, NuoE, NuoF, NuoG, and NuoI. The membranes (10 μg of protein per lane) were loaded on a 13% Laemmli SDS polyacrylamide gel. After electrophoresis, the proteins were transferred to nitrocellulose membranes, and Western blotting was carried out as described in Figure 3.

Effects of NuoJ Mutation on the NDH-1 Activity. We then measured electron-transfer activities of mutant *E. coli* membranes and summarized the results in Table 2. In good agreement with the previous assembly experiments, membranes of all point mutants displayed the dNADH-$K_3Fe(CN)_6$ reductase activity comparable to that of the wild-type. Thus, the mutations introduced into the membrane subunit NuoJ apparently did not affect the intactness of peripheral domain subunits.

By contrast, dNADH oxidase activity and dNADH-DB reductase activity were affected to varied degrees among the mutants. It should be noted that these two activities behaved in a parallel fashion among the mutants tested. The KO-rev mutant exhibited virtually the same properties as the wild-type strain. The complete restoration of the activity to the level of the parental MC4100 strain once again demonstrated that the homologous recombination procedure adopted here did not introduce polar effects on the genes downstream of *nuoJ*. The most dramatic effect on the dNADH oxidase/DB reductase activities was observed with mutation of the conserved residue Val-65. Replacing this residue with a Leu and a Gly resulted in, respectively, an ~80 and ~90% loss of the activities. Less drastic but still significant diminution of the activities occurred with mutations at the Tyr-59, Gly-61, Met-64, and Glu-80 positions. Tyr-59 is well-conserved, and the corresponding position in human ND6 subunit is associated with LHON. Mutations in this position diminished the activities by 42−52%. The two mutants of Glu-80, E80Q and E80A, exhibited small but measurable differences in the NDH-1 activities. While exchanging this acidic residue for the corresponding amide had virtually no effect, replacing it with a nonpolar Ala resulted in an activity loss of ~15%. Apparently, the negative charge at this position does not seem be essential for the function. The G61V mutant exhibited a more significant reduction (~50%) of the energy-transducing NDH-1 activities than the G61L mutant (~30%). A similar result was obtained with the mutation of Met-64, the residue mimicking the human ND6(T14484C) mutation. The M64I mutant had activities close to those from the wild-type strain, while M64V had detectably lower activities.

Table 2: Enzyme Activities of the Membrane-Bound NDH-1 of *E. coli* Wild-Type and Various NuoJ Mutants

	NDH-1 activities[a]			
	dNADH-O_2		dNADH-DB	dNADH-$K_3Fe(CN)_6$
NuoJ mutant	nmol dNADH/ mg protein/min	I_{50} (Cap-40)[b] in μM	nmol dNADH/ mg protein/min	nmol $K_3Fe(CN)_6$/ mg protein/min
wild	478 (100%)	0.12	576 (100%)	1268 (100%)
KO	5 (1%)		29 (5%)	165 (13%)
KO-rev	485 (101%)	0.12	585 (102%)	1283 (101%)
Y59C	277 (58%)	0.11	331 (57%)	1208 (95%)
Y59F	239 (50%)	0.11	274 (48%)	1298 (102%)
G61V	230 (48%)	0.10	305 (53%)	1255 (99%)
G61L	328 (69%)	0.11	412 (72%)	1242 (98%)
M64V	404 (85%)	0.10	512 (89%)	1222 (96%)
M64I	494 (103%)	0.11	612 (106%)	1352 (107%)
V65G	61 (13%)	0.11	69 (12%)	1260 (99%)
V65L	99 (21%)	0.11	133 (23%)	1245 (98%)
F67A	393 (82%)	0.12	493 (86%)	1308 (103%)
E80Q	476 (100%)	0.13	592 (103%)	1279 (101%)
E80A	404 (85%)	0.10	510 (89%)	1294 (102%)

[a] Activities were average values of at least three measurements. The assays were conducted at 37 °C. [b] The concentration of capsaicin-40 that causes 50% inhibition.

Cap-40 is a complex I inhibitor with the binding site located within the membrane domain of the complex. According to Satoh et al. (*33*), cap-40 works as a competitive inhibitor for quinone in the NDH-1/complex I and represses only the energy-coupled activity. In the wild-type strain, cap-40 at 10 μM in the reaction medium inhibited 97% of dNADH oxidase activity and 92% of dNADH-DB reductase activity (data not shown). As shown in Table 2, the I_{50} of cap-40 was unaffected in all the point mutants tested. This finding indicated that none of the point mutants constructed caused any major defects in the cap-40 binding site of NDH-1. If this inhibitor shares a common binding pocket with quinone as reported (*40*, *41*), our result may suggest that

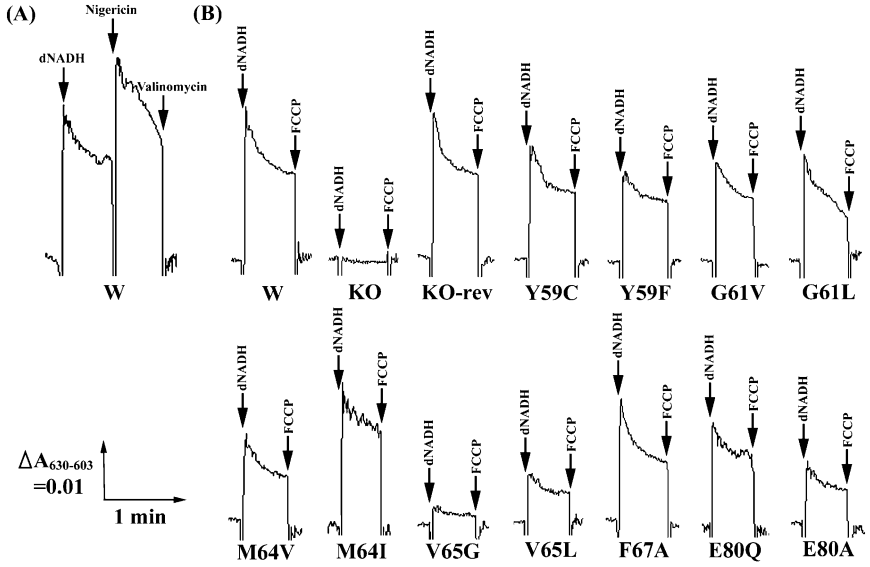

FIGURE 5: Detection of the membrane potential generated by dNADH oxidation in *E. coli* NuoJ mutants. Membranes were prepared from each of the constructed mutants, and the membrane potential was monitored by the absorbance change at the wavelength pair of 630 minus 603 nm at 37 °C. At the time indicated by arrows, 0.2 mM dNADH, 2 μM valinomycin, 0.2 μM nigericin, or 2 μM FCCP was added to the assay mixture containing 50 mM MOPS (pH 7.3), 10 mM $MgCl_2$, 50 mM KCl, 2 μM oxonol VI, and *E. coli* membrane samples (400 μg of protein/mL).

the NuoJ subunit, or more precisely, the residues mutated in this study, is not involved in quinone binding.

Membrane Potential. Using *E. coli* membrane preparations, we have measured membrane potential induced by NDH-1 with oxonol VI as a reporter. As illustrated in Figure 5A, initiation of respiration by the addition of dNADH caused a rapid absorbance increase of oxonol VI at 630 minus 603 nm indicating a formation of energy-dependent membrane potential (positive inside). A subsequent addition of nigericin, an ionophore that catalyzes electroneutral exchange of K^+ for H^+ and thus specifically collapses the ΔpH component of protonmotive force, transiently enhanced the oxonol VI response. The oxonol signal was then entirely abolished by addition of valinomycin, an ionophore that selectively increases the K^+ permeability of the membrane and thus collapses the $\Delta\Psi$ component of the protonmotive force. The absorbance change of oxonol VI generated by dNADH oxidation was measured with mutant *E. coli* membranes (Figure 5B). As expected, the KO-rev mutant showed a response equivalent to the wild-type, both of which were completely reversed by addition of an uncoupler, FCCP. Interestingly, V65G generated very little membrane potential, and its moderately mutated twin, V65L, as well as M64V and E80A had a slightly higher absorbance change but was still much lower than that of the wild-type strain. In contrast, membranes from M64I and F67A had a membrane potential comparable to that of the wild-type strain, while those from Y59C, Y59F, G61V, G61L, and E80Q were all lower to some degree than that of the wild-type strain. Basically the same results were obtained when DB was used as the electron acceptor (data not shown).

Proton Translocation. Fluorescent dye, ACMA, has been used extensively for monitoring the pH gradient across biological membranes. As seen in Figure 6A for the wild-type *E. coli* membranes, the ACMA fluorescence was quenched upon addition of dNADH (acidic inside), and the degree of quenching reached its maximum in the presence of valinomycin. Addition of nigericin abolished the ACMA quenching as expected. ACMA quenching of the mutant *E. coli* membranes is shown in Figure 6B. In both the wild-type strain and the KO-rev mutant, the degree of quenching was nearly 80%. This response was completely repealed by the addition of FCCP. The most striking effect was seen with the Val-65 mutants: V65G did not show any sign of proton translocation, and V65L exhibited 38% quenching. Membranes from G61V, G61L, M64V, and E80A showed a quenching ranging from 56 to 64%. Mutants Y59C, Y59F, M64I, F67A, and E80Q had about the same quenching as the wild-type (data not shown). Similar results were observed when DB was used as the electron acceptor (data not shown).

DISCUSSION

In the present study, we have constructed a series of site-directed point mutants of the NuoJ subunit of *E. coli* NDH-1 (ND6 of complex I) to investigate possible functional roles of this membrane domain subunit. All these mutants exhibited a fully assembled and stable NDH-1 as demonstrated by BN−PAGE, and the dNADH-$K_3Fe(CN)_6$ reductase activity was comparable to that of the wild-type strain. This may not be surprising because replacing a single residue in a membrane domain subunit is unlikely to cause a drastic structural change in the whole complex. Nevertheless, it is important to know that none of the point mutations introduced in this study leads to gross alteration of the whole NDH-1. Therefore, the observed effects of mutations on the energy-coupled activities, namely, the dNADH oxidase and dNADH-DB reductase activities, were the result of impaired catalytic efficiency rather than an incomplete assemble of the enzyme complex or a lack of stability of the NDH-1 complex.

Among the seven mtDNA-encoded subunits of complex I, ND6 is one of the most frequently affected subunits by mutations that are linked to human diseases. Interestingly, most of pathogenic mutations that have been associated with human diseases are clustered within or near TM3. In particular, two residues, Tyr-59 and Met-64, are known to

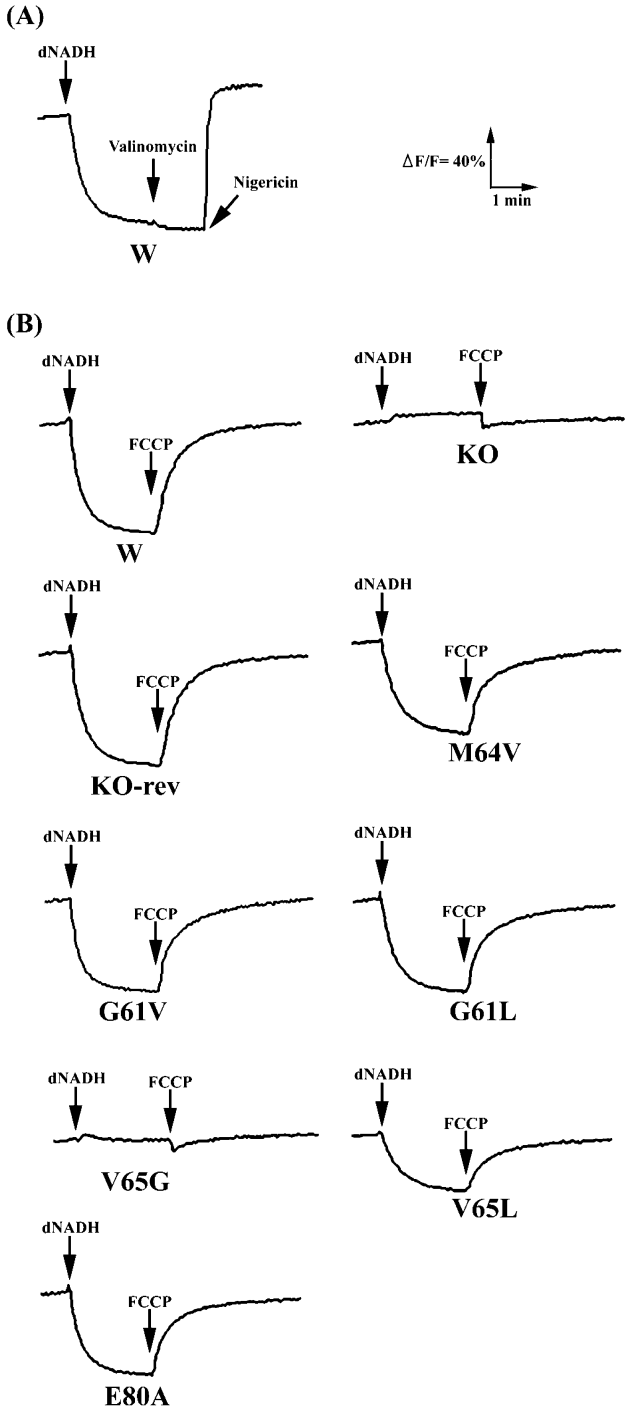

FIGURE 6: Generation of a pH gradient by dNADH oxidation in *E. coli* NuoJ mutants. Membranes were prepared from each of the constructed mutants, and the extent of proton translocation was measured by the quenching of the fluorescence of ACMA at room temperature with an excitation wavelength of 410 nm and an emission wavelength of 480 nm. At the time indicated by arrows, 0.2 mM dNADH, 2 μM valinomycin, 2 μM nigericin, or 10 μM FCCP was added to the assay mixture containing 50 mM MOPS (pH 7.3), 10 mM $MgCl_2$, 50 mM KCl, 2 μM ACMA, and *E. coli* membrane samples (150 μg of protein/mL).

be linked to LHON (*19*). Tyr-59 is an evolutionarily conserved residue with protonable function that lies within TM3. Mutations of this residue (Y59C and Y59F) resulted in a significant inhibition (~40−50%) of the energy-transducing NDH-1 activities as well as reduced membrane potential. Met-64 is also in TM3 but is poorly conserved among species. Both in vitro and in vivo biochemical studies on this mutation showed conflicting results regarding the extent of complex I dysfunction in LHON (*19*). In the present study, the M64V mutant that is equivalent to the LHON primary mutation T14484C (M → V) exhibited slightly lower energy-coupled activities and a moderate reduction in proton translocation and membrane potential.

In the amino acid sequence of the ND6 subunit, the region around TM3 is phylogenetically most conserved. We have mutated highly conserved residues in this region. The most striking alteration of the activities occurred with the Val-65 mutation. A large fraction of the coupled electron-transfer activity was lost in both V65G (~90%) and V65L (~80%). Diminution of membrane potential and proton gradient almost paralleled the decrease in the electron transfer activities. The profound impact of V65G mutation is manifested by its total loss of proton translocation. Because unprotonable residues such as valine are not likely to participate in proton pumping directly, it may be speculated that they contribute to a channel that transfers protons across the membrane. In the case of *E. coli* transhydrogenase, it was reported that four essential, conserved residues, His-91, Ser-139, Asn-222, and Gly-252, appear in four separate transmembrane segments of domain II of the β-subunit of the enzyme that make up a four-helix bundle proton channel and are involved in proton translocation (*42*). It is possible that a similar mechanism exists in the NDH-1. We have recently investigated two carboxyl residues, Asp-79 and Glu-81, located in the middle of TM2 of the *E. coli* NuoA subunit (ND3 of complex I) and found that mutations simultaneously introduced at these two positions almost completely abolished the NDH-1 activities (*26*). In addition, two carboxyl residues, Glu-36 and Glu-72, located in TM2 and TM3, respectively, of the *E. coli* NuoK subunit (ND4L of complex I) have also been shown to behave in a similar manner (*43*). Although relative positions of the three subunits, NuoA, NuoK, and NuoJ, are not known at this moment, it is tempting to envision that they together provide a channel for proton conductance as reported for the proton channel of the transhydrogenase. It should also be considered that removing a hydrophobic side chain in the membrane segment might have a high impact on the local structure. For example, it was reported that dimerization of the transmembrane domain of glycophorin A is mediated by a sequence motif that includes two essential valine residues (*44*). Val-65 of the NuoJ/ND6 subunit is highly conserved, and interestingly, it is located immediately following the residue of the LHON primary mutation (M64V). As we suggested before (*13*), modifications in this region, particularly in TM3, might influence the packing of the putative membrane-spanning helices. The possibility of such alteration of the structure of the transmembrane helices has been suggested for ND6 based on homology-based modeling and computational prediction (*45*).

It is conceivable that site-directed mutation studies targeting at conserved amino acids as well as the residues related to human diseases help us to clarify possible roles of membrane domain subunits on the activity and the assembly of NDH-1. The work presented here is the first of such approaches applied to the ND6 subunit and should be expandable to other subunits that are known to be clinically important in mitochondrial complex I.

ACKNOWLEDGMENT

We thank Dr. Marta Perego (The Scripps Research Institute) for chromosomal DNA manipulation and Drs. Byoung Boo Seo and Tetsuo Yamashita for discussion. This is publication 16809-MEM from The Scripps Research Institute, La Jolla, CA.

REFERENCES

1. Yagi, T., and Matsuno-Yagi, A. (2003) The proton-translocating NADH-quinone oxidoreductase in the respiratory chain: The secret unlocked, *Biochemistry 42*, 2266−2274.
2. Yagi, T., Yano, T., Di Bernardo, S., and Matsuno-Yagi, A. (1998) Procaryotic complex I (NDH-1), an overview, *Biochim. Biophys. Acta 1364*, 125−133.
3. Friedrich, T., Abelmann, A., Brors, B., Guénebaut, V., Kintscher, L., Leonard, K., Rasmussen, T., Scheide, D., Schlitt, A., Schulte, U., and Weiss, H. (1998) Redox components and structure of the respiratory NADH:ubiquinone oxidoreductase (complex I), *Biochim. Biophys. Acta 1365*, 215−219.
4. Guénebaut, V., Schlitt, A., Weiss, H., Leonard, K., and Friedrich, T. (1998) Consistent structure between bacterial and mitochondrial NADH:ubiquinone oxidoreductase (complex I), *J. Mol. Biol. 276*, 105−112.
5. Takano, S., Yano, T., and Yagi, T. (1996) Structural studies of the proton-translocating NADH-quinone oxidoreductase (NDH-1) of *Paracoccus denitrificans*: Identity, property, and stoichiometry of the peripheral subunits, *Biochemistry 35*, 9120−9127.
6. Yano, T., and Yagi, T. (1999) H^+-translocating NADH-quinone oxidoreductase (NDH-1) of *Paracoccus denitrificans*: Studies on topology and stoichiometry of the peripheral subunits, *J. Biol. Chem. 274*, 28606−28611.
7. Friedrich, T. (1998) The NADH:ubiquinone oxidoreductase (complex I) from *Escherichia coli*, *Biochim. Biophys. Acta 1364*, 134−146.
8. Di Bernardo, S., and Yagi, T. (2001) Direct interaction between a membrane domain subunit and a connector subunit in the H^+-translocating NADH-quinone oxidoreductase, *FEBS Lett. 508*, 385−388.
9. Kao, M.-C., Matsuno-Yagi, A., and Yagi, T. (2004) Subunit Proximity in the H^+-Translocating NADH-Quinone Oxidoreductase Probed by Zero-Length Cross-Linking, *Biochemistry 43*, 3750−3755.
10. Yano, T., Magnitsky, S., Sled', V. D., Ohnishi, T., and Yagi, T. (1999) Characterization of the putative 2x[4Fe-4S] binding NQO9 subunit of the proton-translocating NADH-quinone oxidoreductase (NDH-1) of *Paracoccus denitrificans*: Expression, reconstitution, and EPR characterization, *J. Biol. Chem. 274*, 28598−28605.
11. Di Bernardo, S., Yano, T., and Yagi, T. (2000) Exploring the membrane domain of the reduced nicotinamide adenine dinucleotide-quinone oxidoreductase of *Paracoccus denitrificans*: Characterization of the NQO7 subunit, *Biochemistry 39*, 9411−9418.
12. Kao, M.-C., Di Bernardo, S., Matsuno-Yagi, A., and Yagi, T. (2002) Characterization of the membrane domain Nqo11 subunit of the proton-translocating NADH-quinone oxidoreductase of *Paracoccus denitrificans*, *Biochemistry 41*, 4377−4384.
13. Kao, M.-C., Di Bernardo, S., Matsuno-Yagi, A., and Yagi, T. (2003) Characterization and topology of the membrane domain Nqo10 subunit of the proton-translocating NADH-quinone oxidoreductase of *Paracoccus denitrificans*, *Biochemistry 42*, 4534−4543.
14. Chomyn, A., Mariottini, P., Cleeter, M. W. J., Ragan, C. I., Matsuno-Yagi, A., Hatefi, Y., Doolittle, R. F., and Attardi, G. (1985) Six unidentified reading frames of human mitochondrial DNA encode components of the respiratory-chain NADH dehydrogenase, *Nature 314*, 591−597.
15. Chomyn, A., Cleeter, M. W. J., Ragan, C. I., Riley, M., Doolittle, R. F., and Attardi, G. (1986) URF6, last unidentified reading frame of human mtDNA, codes for an NADH dehydrogenase subunit, *Science 234*, 614−618.
16. Nakamaru-Ogiso, E., Sakamoto, K., Matsuno-Yagi, A., Miyoshi, H., and Yagi, T. (2003) The ND5 subunit was labeled by a photoaffinity analogue of fenpyroximate in bovine mitochondrial complex I, *Biochemistry 42*, 746−754.
17. Gong, X., Xie, T., Yu, L., Hesterberg, M., Scheide, D., Friedrich, T., and Yu, C. A. (2003) The ubiquinone-binding site in NADH: ubiquinone oxidoreductase from *Escherichia coli*, *J. Biol. Chem. 278*, 25731−25737.
18. Steuber, J. (2003) The C-terminally Truncated NuoL Subunit (ND5 Homologue) of the Na^+-dependent Complex I from *Escherichia coli* Transports Na^+, *J. Biol. Chem. 278*, 26817−26822.
19. Janssen, R. J., Van den Heuvel, L. P., and Smeitink, J. A. (2004) Genetic defects in the oxidative phosphorylation (OXPHOS) system, *Expert. Rev. Mol. Diagn. 4*, 143−156.
20. Chinnery, P. F., Brown, D. T., Andrews, R. M., Singh-Kler, R., Riordan-Eva, P., Lindley, J., Applegarth, D. A., Turnbull, D. M., and Howell, N. (2001) The mitochondrial ND6 gene is a hot spot for mutations that cause Leber's hereditary optic neuropathy, *Brain 124*, 209−218.
21. Wallace, D. C. (1994) Mitochondrial DNA sequence variation in human evolution and disease, *Proc. Natl. Acad. Sci. U.S.A. 91*, 8739−8746.
22. Bai, Y. D., and Attardi, G. (1998) The mtDNA-encoded ND6 subunit of mitochondrial NADH dehydrogenase is essential for the assembly of the membrane arm and the respiratory function of the enzyme, *EMBO J. 17*, 4848−4858.
23. Cardol, P., Matagne, R. F., and Remacle, C. (2002) Impact of Mutations Affecting ND Mitochondria-encoded Subunits on the Activity and Assembly of Complex I in Chlamydomonas. Implication for the Structural Organization of the Enzyme, *J. Mol. Biol. 319*, 1211−1221.
24. Murphy, E., Huwyler, L., and Freire Bastos, M. C. (1985) Transposon Tn554: complete nucleotide sequence and isolation of transposition-defective and antibiotic-sensitive mutants, *EMBO J. 4*, 3357−3365.
25. Link, A. J., Phillips, D., and Church, G. M. (1997) Methods for generating precise deletions and insertions in the genome of wild-type *Escherichia coli*: application to open reading frame characterization, *J. Bacteriol. 179*, 6228−6237.
26. Kao, M.-C., Di Bernardo, S., Perego, M., Nakamaru-Ogiso, E., Matsuno-Yagi, A., and Yagi, T. (2004) Functional roles of four conserved charged residues in the membrane domain subunit NuoA of the proton-translocating NADH-quinone oxidoreductase from *Escherichia coli*, *J. Biol. Chem. 279*, 32360−32366.
27. Nakamaru-Ogiso, E., Yano, T., Yagi, T., and Ohnishi, T. (2005) Characterization of the iron−sulfur cluster N7(N1c) in the subunit NuoG of the proton-translocating NADH-quinone oxidoreductase from *Escherichia coli*, *J. Biol. Chem. 280*, 301−307.
28. Han, A.-L., Yagi, T., and Hatefi, Y. (1989) Studies on the Structure of NADH:Ubiquinone Oxidoreductase Complex: Topography of the Subunits of the Iron−Sulfur Protein Component, *Arch. Biochem. Biophys. 275*, 166−173.
29. Laemmli, U. K. (1970) Cleavage of structural proteins during the assembly of the head of bacteriophage T4, *Nature 227*, 680−685.
30. Schagger, H., and Von Jagow, G. (1991) Blue native electrophoresis for isolation of membrane protein complexes in enzymatically active form, *Anal. Biochem. 199*, 223−231.
31. Matsushita, K., Ohnishi, T., and Kaback, H. R. (1987) NADH-ubiquinone oxidoreductases of the *Escherichia coli* aerobic respiratory chain, *Biochemistry 26*, 7732−7737.
32. Yagi, T. (1986) Purification and characterization of NADH dehydrogenase complex from *Paracoccus denitrificans*, *Arch. Biochem. Biophys. 250*, 302−311.
33. Satoh, T., Miyoshi, H., Sakamoto, K., and Iwamura, H. (1996) Comparison of the inhibitory action of synthetic capsaicin analogues with various NADH:ubiquinone oxidoreductases, *Biochim. Biophys. Acta 1273*, 21−30.
34. Amarneh, B., and Vik, S. B. (2003) Mutagenesis of Subunit N of the *Escherichia coli* Complex I. Identification of the Initiation Codon and the Sensitivity of Mutants to Decylubiquinone, *Biochemistry 42*, 4800−4808.
35. Fearnley, I. M., and Walker, J. E. (1992) Conservation of sequences of subunits of mitochondrial complex I and their relationships with other proteins, *Biochim. Biophys. Acta 1140*, 105−134.
36. Krogh, A., Larsson, B., Von Heijne, G., and Sonnhammer, E. L. L. (2001) Predicting trnasmembrane protein topology with a hidden Markov model: Application to complete genomes, *J. Mol. Biol. 305*, 567−580.
37. Tusnády, G. E., and Simon, I. (2001) The HMMTOP transmembrane topology prediction server, *Bioinformatics 17*, 849−850.
38. Claros, M. G., and Von Heijne, G. (1994) TopPred II: An improved software for membrane protein structure predictions, *Comput. Appl. Biosci. 10*, 685−686.

39. Hofmann, K., and Stoffel, W. (1993) TMbase—A database of membrane spanning proteins segments, *Biol. Chem. Hoppe-Seyler 374*, 166.
40. Okun, J. G., Lummen, P., and Brandt, U. (1999) Three classes of inhibitors share a common binding domain in mitochondrial complex I (NADH:ubiquinone oxidoreductase), *J. Biol. Chem. 274*, 2625−2630.
41. Shimomura, Y., Kawada, T., and Suzuki, M. (1989) Capsaicin and its analogues inhibit the activity of NADH-coenzyme Q oxidoreductase of the mitochondrial respiratory chain, *Arch. Biochem. Biophys. 270*, 573−577.
42. Yamaguchi, M., and Stout, C. D. (2003) Essential glycine in the proton channel of *Escherichia coli* transhydrogenase, *J. Biol. Chem. 278*, 45333−45339.
43. Kervinen, M., Patsi, J., Finel, M., and Hassinen, I. E. (2004) A Pair of Membrane-Embedded Acidic Residues in the NuoK Subunit of *Escherichia coli* NDH-1, a Counterpart of the ND4L Subunit of the Mitochondrial Complex I, Are Required for High Ubiquinone Reductase Activity, *Biochemistry 43*, 773−781.
44. Liu, W., Crocker, E., Siminovitch, D. J., and Smith, S. O. (2003) Role of side-chain conformational entropy in transmembrane helix dimerization of glycophorin A, *Biophys. J. 84*, 1263−1271.
45. DeHaan, C., Habibi-Nazhad, B., Yan, E., Salloum, N., Parliament, M., and Allalunis-Turner, J. (2004) Mutation in mitochondrial complex I ND6 subunit is associated with defective response to hypoxia in human glioma cells, *Mol. Cancer 3*, 19.
46. Devereux, J., Haeberli, P., and Smithies, O. (1984) A comprehensive set of sequence analysis programs for the VAX, *Nucleic Acids Res. 12*, 387−395.

BI0476477